Proceedings of the Canadian Society for Mechanical Engineering International Congress
32nd Annual Conference of the Computational Fluid Dynamics Society of Canada
Canadian Society of Rheology Symposium
CSME-CFDSC-CSR 2025
May 25–28, 2025, Montréal, Québec, Canada

Non singular integral terminal sliding mode drive anti-skid control based on fuzzy road recognition

Chengyuan Yang[1], Wei Gao[1,2*], Zhaoweng Deng[1,2], Yuping He[3]
[1]School of Automotive Engineering, Hubei University of Automotive Technology, Shiyan, China
[2]College of Energy and Power Engineering, Nanjing University of Aeronautics and Astronautics,Nanjing, China
[3]Department of Automotive and Mechatronics Engineering, University of Ontario Institute of Technology, Oshawa, Canada

Abstract—In order to improve the stability and acceleration of distributed drive electric semi-trailer trains under low adhesion coefficient road surface, an anti-skid control regulation method based on fuzzy road surface recognition algorithm and non-singular integral terminal sliding mode strategy is proposed and devised. In this paper, the vehicle model of the distributed drive electric semi-trailer train is established, and the fuzzy road surface recognition strategy is designed according to the relationship between the adhesion coefficient and the slip ratio, the non-singular integral terminal sliding mode controller is further developed to realize the fast tracking of the slip ratio with the goal of obtaining the optimal slip ratio. The effectiveness of the control strategy is verified by MATLAB-Simulink co-simulation, and the simulation results show that the designed control strategy can quickly and accurately identify the optimal slip ratio under various typical road conditions, and make the wheel slip ratio close to the optimal slip ratio in a short period of time, Therefore,the driving stability and acceleration performance of the vehicle are effectively improved.

Keywords-distributed drive electric semi-trailer train; fuzzy road recognition;non singular integral terminal sliding mode;anti-skid control

I. INTRODUCTION

In recent years, distributed electric drive technology has become a hot topic in vehicle dynamics research, and received more and more attention [1]. Since the distributed drive electric vehicles have a drive motor for each drive wheel, therefore, compared with the conventional centralized drive vehicles, it has the advantages of compact structure, high power transmission efficiency and fast response speed [2]. With the continuous increase of car ownership, all countries in the world are facing serious environmental pollution and non-renewable energy consumption problems. Therefore, the traditional automobile industry continues to upgrade, and so far, the automobile industry has been close to the new energy direction, and the road freight industry is no exception. Semi-trailer trains have the characteristics of high efficiency and large loading capacity. Their proportion of semi-trailer trains in freight vehicles is increasing year by year, and they play an important role in modern highway logistics and transportation. Thus, it is of great significance to combine distributed electric drive technology and semi-trailer trains to create a low-carbon, environmentally friendly, efficient and safe electric drive semi-trailer train.

Anti-skid control is critical to the longitudinal dynamics control of the vehicles, which can effectively improve the vehicle stability [3]. Various control algorithms were proposed and designed to address the problem of poor driving stability of vehicles on low adhesion road surface. Du et al. designed a logic threshold-based anti-skid controller to solve the driving wheel skid of distributed-drive electric vehicles. Simulation results show that the designed controller is highly reliable and achieves the goal of anti-skid [4]. Vasiljevic et al. proposed an anti-skid control strategy for real-time estimation of road conditions using PID algorithm and feed-forward control to control the slip ratio and verified the validity of the anti-skid control strategy [5]. Zhang et al. designed a fuzzy PID-controller for anti-skid control of an electric-driven vehicle [6].

Compared with PID control, sliding mode control (SMC) has also been applied by many researchers in vehicle anti-skid control due to its advantages of fast response, insensitivity to external disturbances, easy implementation and strong robustness [7]. Jeongmin Kim et al. designed a sliding mode controller to control the slip ratio to ensure that the motor outputs the appropriate torque, thereby improving the dynamic performance of the vehicle [8]. Li et al. designed an anti-saturation sliding mode controller with an anti-saturation integral part to control the slip ratio. In addition to the robustness of SMC, the algorithm introduces an integral part to eliminates the steady state error and replaces the sign function with a saturated function, which reduces the chattering in the motor torque, but but the approaching speed of the system state variable is slow [9].

Fund Program:Natural Science Foundation of Hubei Province of China(JCZRLH202500961,2023AFB985), and Schools Unveiling Project (2024JBB02).
About the author:Chengyuan Yang,E-mail:2760702493@qq.com
Corresponding author:Wei Gao, E-mail:gaow_qc@huat.edu.cn

Currently, many anti-skid control methods for distributed drive electric passenger cars were proposed and designed. However, few studies are conducted on the anti-skid control of distributed drive electric semi-trailer trains. In this paper, the fuzzy road identification algorithm is developed to obtain the optimal slip ratio under different road conditions. On this basis, a non-singular integral terminal sliding-mode anti-skid controller for distributed drive electric semi-trailer trains is designed to realize the fast tracking of the wheel slip ratio. Finally, the effectiveness of the anti-skid control strategy is verified by MATLAB/Simulink and TruckSim co-simulation.

II. VEHICLE MODEL

A. TruckSim Model

The 2A CabOver+1A Flatbed Ttl three-axle semi-trailer trains body model in TruckSim software is selected, and the trailer hauls 10 tons of cargo, as shown in Fig. 1, and the whole vehicle is driven by six hub motors, and the power transmission is carried out through the external input method.

Figure 1. Semi-trailer trains body model

B. Motor Model

Because the research focus of this paper is on the anti-skid control of distributed drive electric semi-trailer trains, it is not necessary to establish a complete high-precision motor model. The second-order transfer function is used to represent the relationship between the motor input torque and the actual output torque [10], which can be described as

$$G(s)=\frac{T_d}{T_d^*}=\frac{1}{1+2\zeta s+2\zeta^2 s^2} \tag{1}$$

where T_d is the output torque of the hub motor; T_d^* is the desired torque of the motor; ζ is the motor characteristic constant.

C. Longitudinal Driver Model

The driver model is divided into longitudinal and lateral driver models, where the lateral driver model outputs the front wheel angle and the longitudinal driver model outputs the total driving torque or braking torque. Since the powertrain system in TruckSim software has been replaced when building the distributed drive electric semi-trailer train model, the speed control module of TruckSim software is no longer applicable. In this section, a longitudinal driver model based on PID control is designed to realize vehicle speed tracking control. The input of the PID controller is the difference between the actual speed of the vehicle and the target speed, and its output is the total driving force required for the vehicle to reach the target speed. Thus, the vehicle can achieve constant speed driving. The block diagram of the longitudinal driver model is shown in Fig. 2.

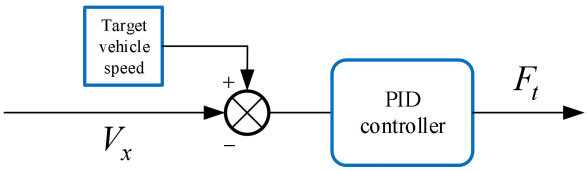

Figure 2. The longitudinal driver model

III. DESIGN AND VALIDATION OF ROAD IDENTIFICATION AGORITHM

A. Wheel Dynamics Model

Because the driving wheel of the distributed drive electric semi-trailer train can be controlled independently, a single wheel model is employed to study the relationship between the driving wheel and the ground, as illustrated in Fig. 3.

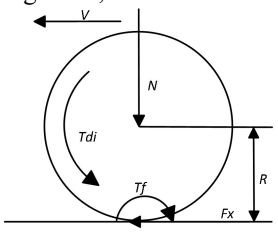

Figure 3. The single-wheel model

To simply calculation, the following assumptions are made: (1) The air resistance and gradient resistance are ignored. (2) The lateral motion and yaw motion of the vehicle are not considered. (3) The left and right wheels have the same physical characteristics. The motion equations of the wheel can be defined as

$$\begin{cases} J_i \dot{w}_i = T_{di} - F_{xi} R \\ T_{fi} = F_{xi} R \end{cases} \tag{3}$$

where J_i is the moment of inertia of the wheel, $\dot{\omega}_i$ is the angular acceleration of the wheel, T_{di} is the driving torque, T_{fi} is the rolling resistance moment, R is the wheel rolling radius , and F_{xi} is the wheel longitudinal force.

The slip ratio of the wheel is defined as

$$\lambda_i=\frac{\omega_i R-v_{xi}}{\omega_i R} \tag{4}$$

where ω_i is the angular speed of the wheel, and v_{xi} is the central speed of the wheel.

The actual utilization adhesion coefficient of the wheel can be expressed as

$$\mu_i=\frac{F_{xi}}{F_{zi}} \tag{5}$$

where F_{xi} and F_{zi} are the longitudinal and vertical forces of the wheel, respectively.

B. Acquisition of the Standard Road Surface Parameters

In order to obtain the optimal slip ratio under different road surface conditions, the algorithm of fuzzy road surface recognition is developed. The establishment of the fuzzy rule needs to input of the maximum utilization adhesion coefficient and the corresponding optimal slip ratio of different standard road surface. In this paper, Burckhardt tyre model is employed to obtain the maximum utilization adhesion coefficient and the optimal slip ratio of the standard road surface. The functional relationship between the adhesion coefficient and slip ratio is expressed as [11]

$$\mu(\lambda) = C_1(1 - e^{-c_2\lambda}) - C_3\lambda \tag{6}$$

where C_1, C_2 and C_3 are the tyre fitting coefficients.

In this paper, eight types road surface are chosen as standard road surfaces. The values of C_1, C_2, C_3, the maximum utilization adhesion coefficient, and the corresponding optimal slip ratio of different road surfaces are shown in Table I. The curves of utilization adhesion coefficient and slip ratio of different road surfaces are depicted in Fig. 4.

TABLE I. PARAMETERS OF BURCKHARDT TYRE MODEL FOR DIFFERENT ROAD SURFACES

Types of Road Surface	C_1	C_2	C_3	λ_{opt}	μ_{max}
Dry asphalt	1.281	23.993	0.520	0.170	1.171
Dry cement	1.196	25.166	0.539	0.160	1.092
Wet asphalt ((low)	1.027	29.494	0.442	0.143	0.950
Wet asphalt (medium)	0.856	33.821	0.345	0.131	0.800
Wet asphalt (high)	0.628	33.765	0.200	0.110	0.600
Cobblestone	0.400	60.01	0.120	0.088	0.386
Snow	0.195	94.129	0.065	0.065	0.190
Ice	0.050	306.39	0.001	0.050	0.050

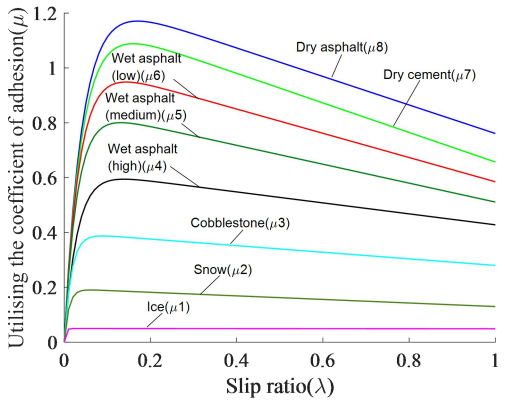

Figure 4. Standard road surface μ-λ curves

C. Algorithm of Fuzzy Road Surface Recognition

In this section, the fuzzy controller is designed to recognize the optimal slip ratio of the current road surface. The inputs of the controller are the actual slip ratio of the driving wheel and the utilization adhesion coefficient, and the output is the similarity between the actual road surface utilization adhesion coefficient and the standard road surface utilization adhesion coefficient. The optimal slip ratio of the current road surface is calculated using the weighted average formula, which is expressed as

$$\lambda_{opt} = \frac{\sum_{j=1}^{8} x_j \lambda_{jopt}}{\sum_{j=1}^{8} x_j} \tag{7}$$

where x_j (j = 1,2,..., 8) is the similarity between the actual road surface utilization adhesion coefficient and the standard road surface utilization adhesion coefficient.

The slip ratio is fuzzified into three subsets, i.e., large, medium and small, and the slip ratio membership function is illustrateded in Fig. 5. According to the difference of wheel slip ratio, three cases are divided, that is small slip ratio, medium slip ratio and large slip ratio. The utilization adhesion coefficients are fuzzified into eight fuzzy subsets: ice, snow, cobblestone, wet asphalt (low), wet asphalt (medium), wet asphalt (high), dry cement, and dry asphalt. The triangular membership function are chosen, as shown in Fig. 6 (a)-(c).

The similarity is fuzzified into totally different(TD), different (D), generally similar (GS), similar (S), extremely similar (ES). The membership function of the similarity is shown in Fig. 7.

The fuzzy levels corresponding to different slip ratios and different road conditions are determined based on the experience of experts. A, B, C, D, E, F, G, and H represent dry asphalt, dry cement, wet asphalt (high), wet asphalt (medium), wet asphalt (low), cobblestone, snow, and ice road surfaces, and the specific fuzzy rules are shown in Table II.

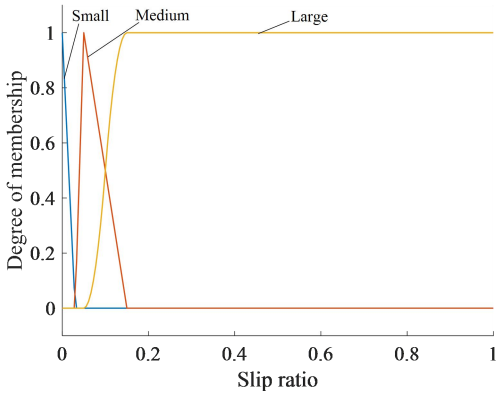

Figure 5. Membership function of silp ratio

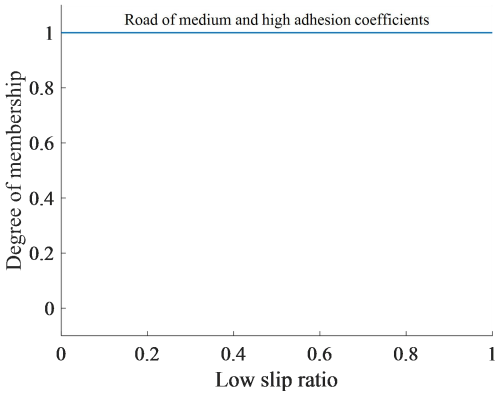

(a)

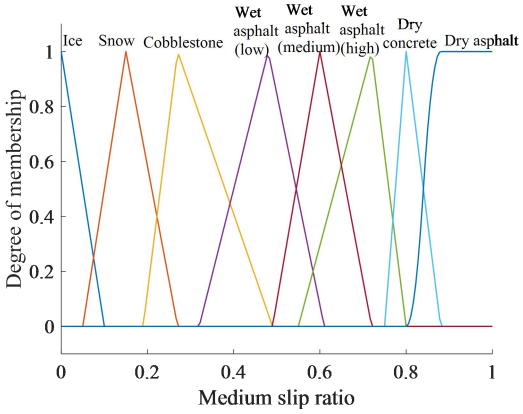

(b)

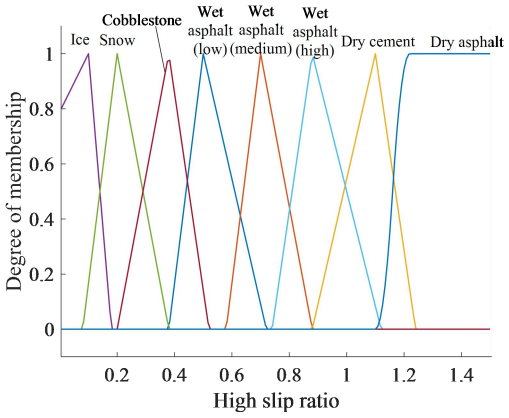

(C)

Figure 6. Membeiship function of utilization adhesion coefficients

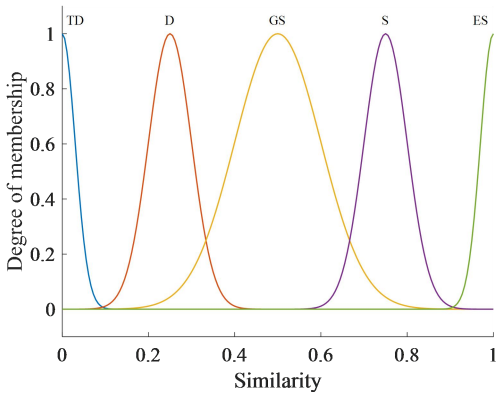

Figure 7. Membership function of similarity

TABLE II. FUZZY RULE

Input		Output							
Slip ratio	Utilization adhesion coefficient	A	B	C	D	E	F	G	H
Large	A	TD	TD	D	GS	GS	GS	S	ES
Large	B	TD	TD	D	GS	GS	S	ES	S
Large	C	TD	TD	TD	GS	S	ES	S	D
Large	D	TD	TD	D	S	ES	S	GS	D
Large	E	TD	TD	GS	ES	S	GS	D	TD
Large	F	D	S	ES	GS	D	TD	TD	TD
Large	G	GS	ES	D	TD	TD	TD	TD	TD
Large	H	ES	D	TD	TD	TD	TD	TD	TD
Medium	A	TD	TD	D	GS	S	S	ES	ES
Medium	B	TD	TD	D	GS	S	S	ES	ES
Medium	C	TD	TD	TD	GS	S	ES	S	S
Medium	D	TD	TD	D	S	ES	S	GS	GS
Medium	E	TD	TD	GS	ES	S	S	TD	TD
Medium	F	D	S	ES	S	D	TD	TD	TD
Medium	G	GS	ES	D	TD	TD	TD	TD	TD
Medium	H	ES	TD	TD	TD	TD	TD	TD	TD
Small	I	TD	TD	TD	TD	ES	ES	ES	ES

D. Fuzzy Road Surface Recognition Verification

As can be seen from the optimal slip ratio identification curve in Fig. 8, the fuzzy road surface identification can better identify the optimal slip ratio, and can quickly estimate the optimal slip ratio of each wheel at about 0.065, with a high degree of accuracy.

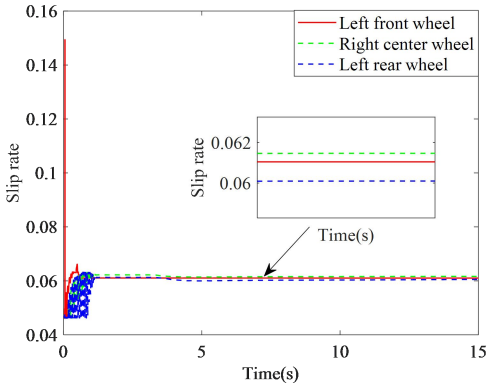

Figure 8. Optimal slip ratio

IV. ANTI-SKID CONTROLLER DESIGN

A. System Structure

The structure of the control algorithm proposed in this paper is shown in Fig. 9. It consists of three parts: longitudinal driver model, fuzzy road surface recognition and driving anti-skid controller. The longitudinal driver model obtains the total driving force required by the vehicle through the difference between the actual speed and the target speed. The wheel slip ratio and the utilised adhesion coefficient are input to the fuzzy controller for road surface identification to obtain the optimal slip ratio and the peak adhesion coefficient, and finally, the deviation of the actual slip ratio from the optimal slip ratio is input to the non-singular integral terminal sliding-mode controller to obtain the required torque of each wheel and to realise the drive anti-skid control.

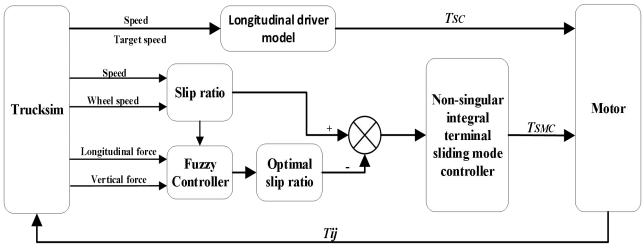

Figure 9. Controller structure.

B. The sliding mode control algorithm

In order to improve the longitudinal acceleration performance and lateral stability of the vehicle, the slip ratio of the wheel need to be controlled near the optimal slip ratio. An anti-skid controller is developed using non-singular integral terminal sliding mode control technique for the distributed drive electric semi-trailer train. The control objective of the non-singular integral terminal sliding mode controller is the difference of the actual slip ratio of the wheel and its optimal slip ratio, which can be defined as

$$e = \lambda - \lambda_0 \tag{8}$$

where λ is the actual slip ratio of the wheel, λ_0 is the optimal slip ratio of the wheel.

In order to reduce the chattering of the sliding mode control system and improve the convergence speed of the system state variables, the non-singular integral terminal sliding mode surface function is defined as

$$S = e(t) + c\int_0^t e(t)^{\frac{p}{q}}\,dt \tag{9}$$

where c is a constant of integration and c>0, p ,*and* q are positive odd numbers and satisfy $1<p/q<2$.

In order to ensure the fast and stable response of the control system, the exponential reaching law is chosen as the reaching law of the system, and its expression is as follows

$$\dot{S} = -\varepsilon_1 \cdot sgn(S) - \varepsilon_2 S \tag{10}$$

where ε_1 and ε_2 are the control coefficients, and $\varepsilon_1>0$, $\varepsilon_2>0$.

To further eliminate the chattering of the control system, the sign function sgn(s) is replaced by the hyperbolic tangent tanh(S) function, which is expressed as

$$\tan h(S) = \frac{e^{s} - e^{-s}}{e^{s} + e^{-s}} \tag{11}$$

The required driving torque of the target wheel is

$$T_{smc} = -\left[c(\lambda-\lambda_0)^{\frac{p}{q}} + \varepsilon_1 \cdot \tanh(S) + \varepsilon_2 S\right] \cdot \frac{I_w \omega^2 r_w}{v_x} + \frac{I_w \omega \dot{v}_x}{v_x} + F_{xi} \cdot r_w \tag{12}$$

where I_w is the moment of inertia of the driving wheel.

V. SIMULATION AND RESULTS

To validate the effectiveness of the anti-skid control strategy, MATLAB/Simulink and TruckSim co-simulation is carried out on the low adhesion road surface with a road adhesion coefficient of 0.2. The vehicle accelerates at full throttle from a standstill to a speed of 80 km/h. The simulation results are shown in Fig. 10(a)-(d).

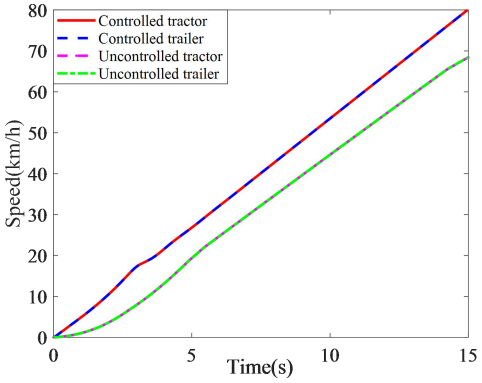

(a) Vehicle speed

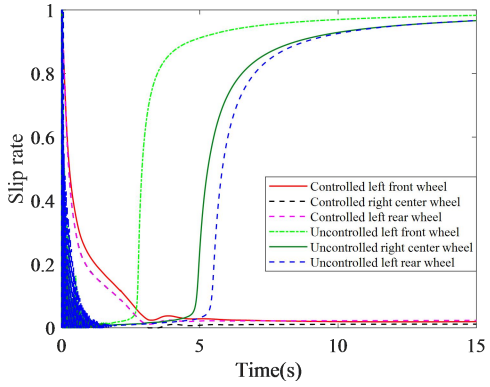

(b) Actual slip ratio

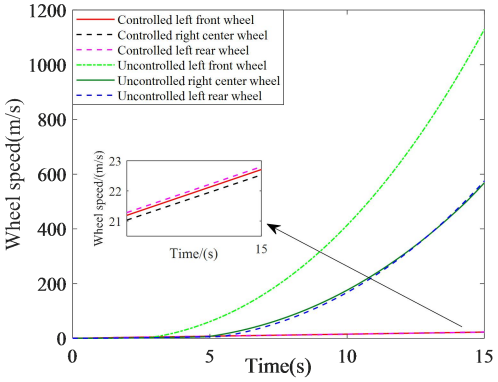

(c) Wheel speed

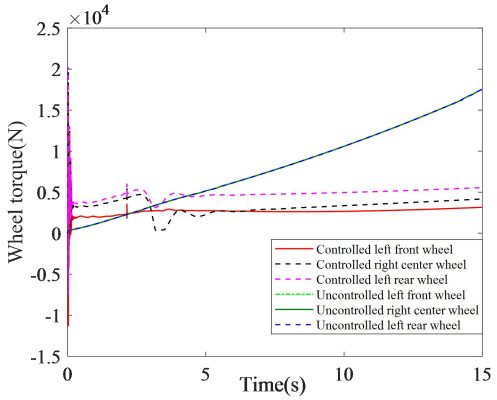

(d) Motor torque curve

Figure 10. Simulation result curve

From the simulation curve of vehicle speed in Fig. 10(a), it can be seen that under the same working condition, the speed tracking effect of tractor and trailer is better than that of the uncontrolled vehicle after adopting the sliding mode control, and the longitudinal attachment coefficient decreases due to the sliding of the wheels, resulting in the deterioration of the speed tracking effect of the uncontrolled vehicle.

From the actual slip ratio curves in Fig. 10(b), it can be seen that all the wheels of the uncontrolled vehicle have a slip ratio of 0.9 or more, and excessive wheel slip occurs. However, the slip-mode-controlled vehicle can quickly control the actual slip ratio near the optimal slip ratio, preventing excessive wheel slip.

From the wheel speed curve in Fig. 10(c), it can be seen that the wheel speed of each wheel increases rapidly in about 3s for the vehicle without driving anti-skid control, and the wheels appear to slip excessively, whereas the wheel speed of each wheel increases gradually with the increase of the vehicle speed for the vehicle with sliding-mode control, but the wheel speed of each wheel stays within 23m/s, and there is no excessive slipping of the wheels.

From the motor torque curve in Fig. 10(d), it can be seen that the motor torque increases as the vehicle speed increases. When the wheel driving torque exceeds the torque that can be provided by the road surface, the slipping phenomenon occurs in each wheel without control, and the torque of each motor increases rapidly. The drive anti-skid control controls the slip ratio of the drive wheels near the optimal slip ratio, so the motor driving torque oscillates around 3s, and then the motor driving torque remains unchanged due to the increase of the vehicle speed when the drive wheel motor reaches the constant power region.

VI. CONCLUSION

This paper designs a non singular integral terminal sliding mode drive anti-skid controller based on fuzzy road surface recognition. Through joint simulation with TruckSim and MATLAB/Simulink, it is verified that the fuzzy road surface recognition designed in this paper can accurately identify the optimal slip ratio of the road. The driving anti-skid controller can control the actual slip ratio of each wheel of the distributed semi-trailer train near the optimal slip ratio, which has a good driving anti-skid effect and prevents excessive slip of each wheel.

VII. ACKNOWLEDGEMENT

This research is financially supported by Natural Science Foundation of Hubei Province Joint Fund Project (JCZRLH202500961),Natural Science Foundation of Hubei Province of China (Grant No. 2023AFB985), and Schools Unveiling Project (2024JBB02).

REFERENCES

[1] W. Gao, Y. Liao, Z. Deng, Y. Zhao, and B. Wang, “Study on lateral stability of distributed drive electric tractor semi-trailers under low adhesion road conditions,” Trans. Can. Soc. Mech. Eng, 2024, vol. 2, no. 4, pp. 592-604.

[2] Y. Liu, B. Wang, and Y. He, “Research on electronic differential control strategy of distributed electric drive vehicle based on torque optimal distribution,” Prog. in Can. Mech. Eng, 2021, vol. 4.

[3] Y. Bao, C. Du, D. Wu, H. Liu, W. Liu, and J. Li, “Coordinated slip control of multi-axle distributed drive vehicle based on hlqr,” Mathematics, 2023, vol. 11, no. 8, pp. 1964.

[4] J. Du, D. Yin, J. Wang, and L. Chen, “Anti-skid control of four-wheel hub-driven electric vehicle based on energy method,” IEEE Int. Conf. Mech. Control. Comput. Eng, 2020, vol. 5, pp. 925-930.

[5] G. Vasiljevic, K. Griparic, and S. Bogdan, “Experimental testing of a traction control system with on-line road condition estimation for electric vehicles,” IEEE Medit. Conf. Control. Auto, 2013, vol. 21, pp. 296-302.

[6] C. Zhang, J. Ma, B. Chang, and J. Wang, “Research on anti-skid control strategy for four-wheel independent drive electric vehicle,” World. Elect. Veh. Jour, 2021, vol. 12, no. 3, pp. 150.

[7] S. Zhu, and Y. He . “A Unified Lateral Preview Driver Model for Road Vehicles,” IEEE Trans. Intell, 2020, vol. 21, no. 11, pp. 4858-4868.

[8] J. Kim, C. Park, S. Hwang, Y. Hori, and H. Kim, ″Control algorithm for an independent motor-drive vehicle,″ IEEE Trans. on Veh. Technol. 2010, vol. 59, no. 7, pp. 3213-3222.

[9] B. Li, L. Xiong, and B. Leng, “Adaptive anti-slip regulation method for electric vehicle with in-wheel motors considering the road slope,” IEEE Intell. Veh. Symp, 2018, vol. 4, pp. 1-6.

[10] Q. Chen, W. Xu, Z. Lv, D. Zeng, C. Zhong, and X. Zeng, “Anti-slip regulation method for electric vehicles with four in-wheel motors based on the identification of slip ratio,” Trans. Can. Soc. Mech. Eng. 2023, vol. 48, no. 1, pp. 15-25.

[11] Burckhardt, M.Fahrnverktechnik: Radschlupf Regelsysteme. Vogel-Verlag, 1993, Germany.

Dear Editor-in-Chief

We wish to submit our article “Non singular integral terminal sliding mode drive anti-skid control based on fuzzy road recognition” to be considered for publication in the CSME-CFDSC-CSR 2025 International Congress.

In order to improve the stability and acceleration of distributed drive electric semi-trailer trains under low adhesion coefficient road surface, an anti-skid control regulation method based on fuzzy road surface recognition algorithm and non-singular integral terminal sliding mode strategy is proposed and devised. In this paper, the vehicle model of the distributed drive electric semi-trailer train is established, and the fuzzy road surface recognition strategy is designed according to the relationship between the adhesion coefficient and the slip ratio, the non-singular integral terminal sliding mode controller is further developed to realize the fast tracking of the slip ratio with the goal of obtaining the optimal slip ratio. The effectiveness of the control strategy is verified by MATLAB-Simulink co-simulation, and the simulation results show that the designed control strategy can quickly and accurately identify the optimal slip ratio under various typical road conditions, and make the wheel slip ratio close to the optimal slip ratio in a short period of time, Therefore,the driving stability and acceleration performance of the vehicle are effectively improved.

I am authorized on behalf of all the authors of this article to confirm that no author has any conflict of interest to disclose, all authors have approved the version submitted for publication, the work in this article is original and has not been published previously,and the article is not under consideration by any other journals and conferences.

We thank you for your kind consideration of our article. Please do not hesitate to contact me directly if any further information is required. I look forward to hearing from you.

Yours sincerely

Wei Gao

Associate Professor

1) College of Energy and Power Engineering,Nanjing University of Aeronautics and Astronautics,Nanjing, P.R.China

2) Hubei Key Laboratory of Automotive Power Train and Electronic Control,Hubei University of Automotive Technology, Shiyan, P.R.China

Tel.: +86 13636204878

mail: gaow_qc@huat.edu.cn

gaowei978112@163.com

Dear Editor and Reviewers,

We thank the editors and reviewers for the constructive comments. Your insightful comments and suggestions have significantly strengthened the quality of our work.

In response to the editor’s and reviewers’ recommendations, we have carefully revised the manuscript to address all concerns raised. Detailed point-by-point responses to each comment are provided below, and corresponding revisions are highlighted in yellow within the manuscript for ease of review.

Once again, we extend our heartfelt thanks for your time, expertise, and dedication to improving scholarly work. Please do not hesitate to contact us if further clarifications or adjustments are needed.

With kind regards,

The Authors

➢ Detailed responses to reviewer comments:

***Point* 1:** Page 1: there is a lacking space between “attention” and “[1]”.

Response 1:

We thank the reviewer for this comment. In the revised manuscript, we have added a space between “attention” and “[1]”, please refer to the yellow highlighted in Section I, page 1 of the revised manuscript.

***Point 2*:** Page 1: “Since the distributed drive electric vehicles assign a drive motor to each drive wheel.” is not a sentence. Please reformulate.

Response 2:

Thank you very much for your patience in correcting this, we have made the change in the revised manuscript and highlighted it in yellow. Please refer to the yellow highlighted in Section I, page 1 of the revised manuscript, copied below.

Since the distributed drive electric vehicles have a drive motor for each drive wheel, therefore, compared with the conventional centralized drive vehicles, it has the advantages of compact structure, high power transmission efficiency and fast response speed [2].

***Point 3*:** Page 1: there is a lacking space between “[2].” and “With”.

Response 3:

We thank the reviewers for pointing this out. In the revised manuscript, we have added a space between “[2].” and “With”, please refer to the yellow highlighted in Section I, page 1 of the revised manuscript.

***Point 4*:** Page 1: there is a lacking space between “stability” and “[3]”.

Response 4:

Thank you very much for your valuable comments. In the revised manuscript, we have added a space between “stability” and “[3]”, please refer to the yellow highlighted section on page 1 of the revised manuscript.

***Point 5*:** Page 1: there is a lacking space between “skid” and “[4]”.

Response 5:

We thank the reviewer for pointing out this issue, we have added a space between “skid” and “[4]” and highlighted it in yellow. Please refer to the yellow highlighted in Section I, page 1 of the revised manuscript.

***Point 6*:** Page 1: there is a lacking space between “strategy” and “[5]”.

Response 6:

Thank you very much for your correction. In the revised manuscript, we have added a space between “strategy” and “[5]”, please refer to the yellow highlighted in Section I, page 1 of the revised manuscript.

***Point 7*:** Page 1: “vehicle.[6]” should read “vehicle [6].”.

Response 7:

Thank you very much for your valuable comments. In the revised manuscript, we have changed “vehicle.[6]” to “vehicle [6].”, please refer to the yellow highlighted in Section I, page 1 of the revised manuscript.

***Point 8*:** Page 1: there is a lacking space between “robustness” and “[7]”.

Response 8:

We thank the reviewer for this comment. In the revised manuscript, we have added a space between “robustness” and “[7]”, please refer to the yellow highlighted in Section I, page 1 of the revised manuscript.

***Point 9*:** Page 1: there is a lacking space between “vehicle” and “[8]”.

Response 9:

Thank you very much for your valuable comments. In the revised manuscript, we have added a space between “vehicle” and “[8]”, please refer to the yellow highlighted in Section I, page 1 of the revised manuscript.

***Point 10*:** Page 1: there is a lacking space between “slow” and “[9]”.

Response 10:

Thank you very much for your valuable comments, In the revised manuscript, we have added a space between “slow” and “[9]”, please refer to the yellow highlighted in Section I, page 1 of the revised manuscript.

***Point 11*:** Page 2: there is a lacking space between “torque” and “[10]”.

Response 11:

We thank the reviewers for pointing this out. In the revised manuscript, we have added a space between “torque” and “[10]”, please refer to the yellow highlighted in Section Ⅱ, page 2 of the revised manuscript.

***Point* 12:** Page 3: there is a lacking space between “Fig.” and “5”. The same comments apply below between “Fig.” and “6”.

Response 12:

We thank the reviewer for this comment. In the revised manuscript, we have added a space between “Fig.” and “5” and between “Fig.” and “6”. These changes are highlighted in yellow in Part C (page 3) of the revised manuscript for ease of reference.

***Point 13*:** Pages 3 and 4: Fig. 6 must be put on the same page.

Response 13:

Thank you very much for your valuable comment. In the revised manuscript, we have put Fig. 6 on the same page, please refer to Fig 6, page 4 of the revised manuscript, highlighted in yellow.

***Point 14*:** Page 4: there is a lacking space between “Fig.” and “7”.

Response 14:

We thank the reviewer for pointing out this issue, we have added a space between “Fig.” and “7” and highlighted it in yellow. Please refer to page 3, Part C of the revised manuscript.

***Point 15*:** Page 4: An inset could be of interest to better see the curves obtained during the first s.

Response 15:

We thank the reviewers for pointing this out. In the revised manuscript, we have included an illustration of the curves obtained during the first s for easy reading, as shown in Fig. 8.

***Point 16*:** Page 6: “Fig. 8(b)” and “Fig. 8(d)” should read “Fig. 10(b)” and “Fig. 10(d)”. Please correct.

Response 16:

Thank you very much for your patience in correcting this, it is an issue we overlooked and we apologize for our carelessness. In the revised manuscript, we have made the change on page 6: “Fig 8(b)” and “Fig 8(d)” to “Fig 10(b)” and “Fig 10(d)” as shown in the yellow highlighted section on page 6.